Impedance spectroscopy of suspension plasma sprayed hydroxyapatite coatings

Tomasz PIASECKI[1*], Karol NITSCH[1], Lech PAWŁOWSKI[2], Roman JAWORSKI[2]

[1]Faculty of Microsystem Electronics and Photonics, Wrocław University of Technology,
 Janiszewskiego 11/17, 50-372 Wrocław, Poland

[2]Ecole Nationale Supérieure de Chimie de Lille, Service of Thermal Spraying,
 8 avenue Mendeleiev, B.P. 90108, 59650 Villeneuve d'Ascq Cedex, France

*Corresponding author: tomasz.piasecki@pwr.wroc.pl

Impedance spectroscopy was used to investigate the properties of hydroxyapatite (HA) coatings and their dependence on fabrication parameters. The HA layers were deposited on the titanium substrates using suspension plasma spraying. The analysis of the results was performed using equivalent circuit modelling. The HA layers contained crystalline and amorphous phases. The amount of amorphous phase raised with an increase of plasma torch power. The porosity of coatings was investigated by observation of water evaporation process. The conclusion was that samples fabricated with lower torch power had smaller and more complex pores structure.

Keywords: impedance spectroscopy, hydroxyapatite, suspension, plasma spraying, porosity.

1. Introduction

Hydroxyapatite (HA, chemical formula $Ca_{10}(PO_4)_6(OH)_2$) is a biocompatible ceramics used as coating on metallic (Ti_6Al_4V, Ti or stainless steel) prosthesis of hip, knee joints and dental prosthesis of teeth roots. The atmospheric plasma spraying using coarse powders is the most popular method of HA coating deposition. The application of fine agglomerated crystals dry powders or fine powders suspensions may result in nanostructured coatings, which exhibit better properties than microstructured coatings [1, 2]. Suspension may be injected directly into a plasma generated in conventional plasma torch.

Impedance spectroscopy is one of the methods that may be used to determine sprayed layer properties [3, 4] as it gives information about the material under investigation such as electrical properties, microstructure, defects and their dependence on the measurement conditions.

2. Sample preparation

The fine HA powder was home synthesized. Its grain size distribution is shown in Fig. 1. Suspension contained 20 wt.% of the powder. The solvent was a mixture of water with 50 vol.% ethanol.
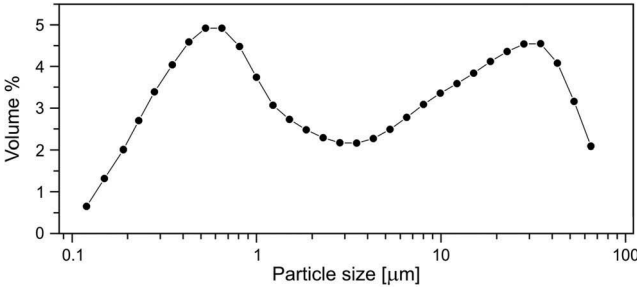

Fig. 1. HA powder grain size distribution.

The substrates were titanium plate with dimensions $20 \times 20 \times 0.5$ mm. The substrates were sand blasted to improve adhesion between the coating and the substrate. The blasting was made using corundum grit (size 250 ± 120 μm), under pressure of 2 bar, then the substrates were cleaned by ethanol and dried by compressed air.

Suspension was injected by a nozzle into the plasma jet inside plasma torch Praxair SG-100, mounted on a 5-axis ABB IRB-6 industrial robot. As plasma gas, a mixture of Ar and H_2 with flow rate of 45 and 5 slpm, correspondingly, was used. The sample crossection (Fig. 2) shows the porous structure of the HA layer.
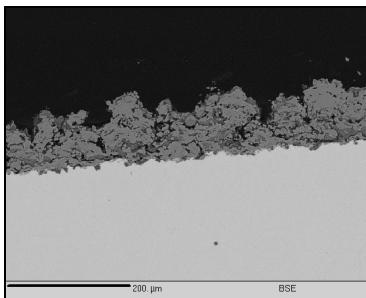

Fig. 2. HA layer crossection (sample 200).

T a b l e 1. Design of experiments.

Experiment	Torch power	Spraying distance	Sample symbol
1	default	default	100
2	–	–	200
3	+	–	300
4	–	+	400
5	+	+	500

   Design of experiments was used to examine the influence of spraying parameters on microstructure of HA coatings. Two levels – and + of electric arc power corresponded to 27 and 33 kW, two levels – and + for spraying distance 50 and 70 mm were chosen. Default experiment was carried out for level 0, *i.e.*, 30 kW and 60 mm. All experimental runs are shown in Tab. 1.

3. Measurement setup

Impedance spectroscopy measurements were performed in the sandwich configuration. The HA layer acted as a dielectric while the electrodes were Ti substrate and silver conducting paint electrode painted on the HA layer. Agilent 4294A impedance analyzer was used. Samples were placed on the heated stage equipped with PID temperature controller. This setup was used to perform two series of measurements.

   In the first measurement, series samples were heated up to 210 °C and kept in that temperature for 30 min to remove moisture. Then, a group of impedance spectra were measured in the frequency range from 40 Hz to 4 MHz at temperatures changing from 210 °C to 30 °C with 30 °C steps. This measurement was performed to obtain information about the dry HA electric properties and their dependence on temperature.

   Second measurement series was performed to determine the porosity of the samples. Samples were immersed for 4 hours in the deionised water at 60 °C to saturate them with water. Then the sample was put on the heated stage at 60 °C and a number of fast, coarse impedance spectra in the frequency range from 200 Hz to 10 MHz were measured as the sample was drying and the water evaporating.

4. Results

4.1. Measurements of dry samples

The temperature dependences of dry HA layers impedance spectra were similar in all the samples. They behaved like lossy capacitor with two dielectric relaxation processes whose time constants (TC_1 and TC_2) depended on the temperature. One dielectric relaxation (TC_1) was visible only at high temperature due to the limitations of impedance spectra bandwidth (Fig. 3).

   The electric equivalent circuit modelling was used to analyze measured spectra. A parallel equivalent circuit [5] was chosen (Fig. 4).

   The equivalent circuit consisted of: R_S, C_{PAR} – parasitic resistance and capacitance of the fixture and electrodes, $C_1 \parallel CPE_1$ – modelled crystalline and amorphous phases in bulk HA, R_{TC_x} – CPE_{TC_x} – modelling dielectric relaxations [6], where the CPE is a constant phase element [7] whose admittance is given by the equation:

$$Y = Q \cdot (j\omega)^n \tag{1}$$

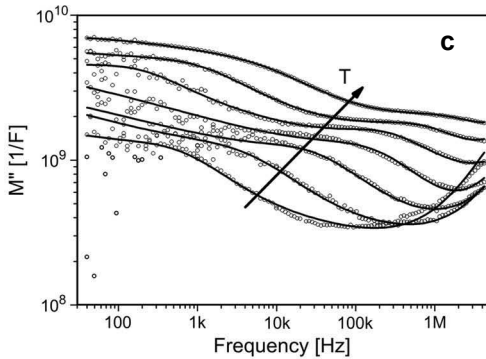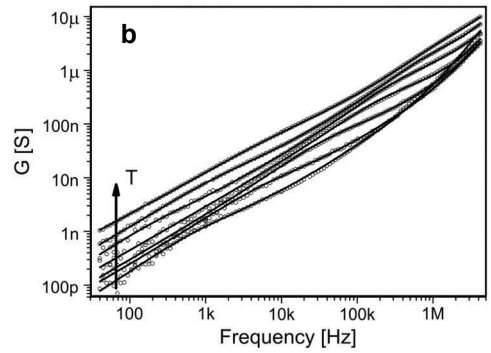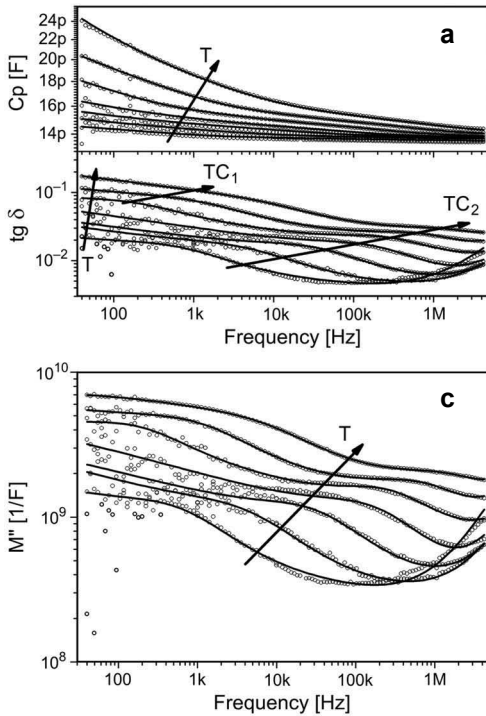Equivalent circuit was fitted to measured spectra at varying temperatures. The results of fitting are shown in Fig. 5.

Fig. 3. Example of measured impedance spectra (sample 100): parallel capacitance and loss factor (**a**), conductivity (**b**), imaginary dielectric modulus (**c**).
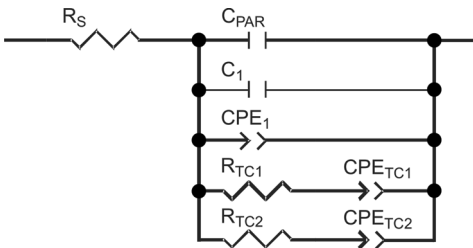

Fig. 4. Equivalent circuit used in HA layer analysis.

The C_1 value remained virtually constant. The CPE$_1$ Q value varied with temperature, however large fitting errors at high temperatures made it impossible to draw any conclusion, but the *n*-factor remained constant. The dielectric relaxation time constants depended on temperature according to the Arrhenius law. It was possible to calculate the activation energy only for TC$_2$ as TC$_1$ was measured only at 3 temperature points.

All samples showed similar behaviour. The results of equivalent circuit analysis are given in Tab. 2. The *n*-factors in the CPE$_1$ and CPE$_{TC_2}$ correspond to the amount of amorphous phase in the HA layer. It's value close to 0.8 is typical of amorphous materials [6]. Samples fabricated with higher torch power contained less crystalline phase in HA layer and more of the amorphous phase. HA layers were highly defective
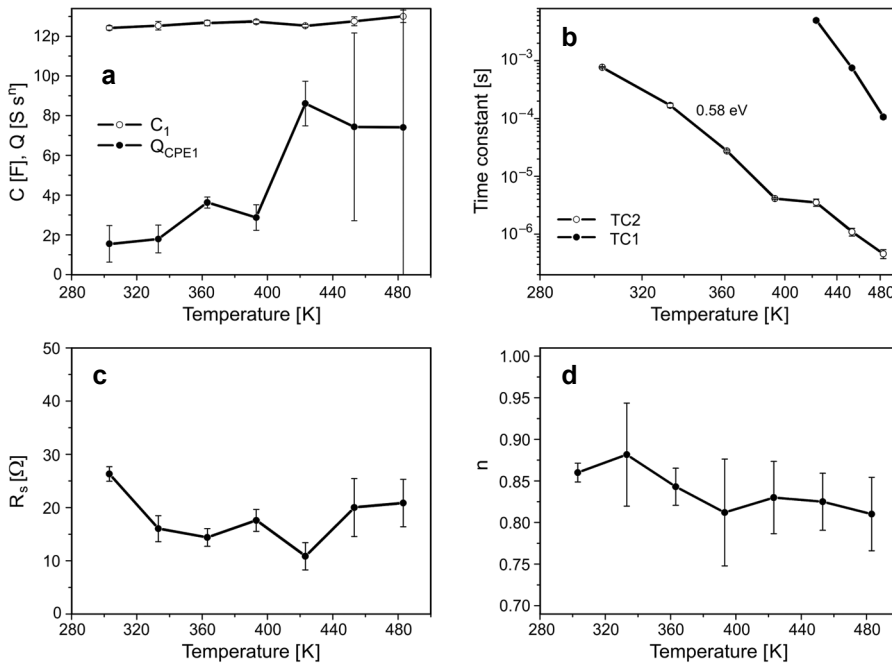
Fig. 5. Temperature dependence of model parameter values (sample 100): C_1 capacitance and CPE_1 Q factor (**a**), Arrhenius plot of time constants of dielectric relaxations (**b**), series resistance (**c**), CPE_1 *n*-factor (**d**). Error bars correspond with fitting error.

T a b l e 2. Results of the impedance spectra analysis: *n*-parameter of CPE_1 element, activation energy E_a of dielectric relaxation TC_2, *n*-parameter of CPE_{TC2} element and drying time of sample.

Sample	CPE_1 *n*	E_a of TC_2 [eV]	CPE_{TC2} *n*	Drying time [s]
100	0.84	0.58	0.75	13.5
200	0.89	0.49	0.82	40.5
300	0.86	0.55	0.83	44.5
400	0.81	0.42	0.71	22.5
500	0.82	0.48	0.72	–

as activation energies of dielectric relaxation in all samples were much lower than 2 eV reported as activation energy of conductivity in bulk HA [8].

4.2. Water absorption measurements

The impedance spectra of wet samples are shown in Fig. 6**a**. At low frequencies strong capacitance dispersion is visible. It was caused by the dielectric polarization in water [9]. As the sample dried out the dispersion shifted to lower frequencies and
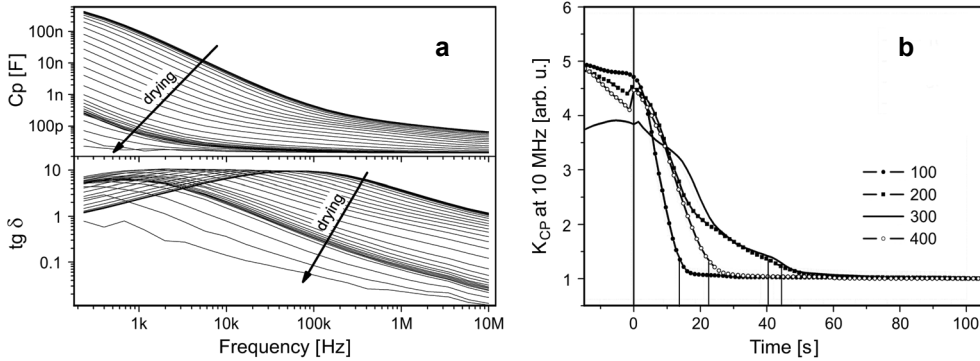
Fig. 6. Changes of impedance spectra while sample drying (**a**), capacitance at 10 MHz normalized to dry sample capacitance (**b**).

disappeared. At high frequencies the changes in capacitance were related mainly to the changes of effective electric permittivity of HA–H$_2$O composition. Changes resulted from large differences in electric permittivities of water ($\varepsilon_{H_2O} = 67$ at 60 °C [10]) and dry hydroxyapatite ($\varepsilon_{HA} = 18$ [8]).

The time equal 0 was the moment at which the impedance spectra of wet sample started to change due to the water evaporation. To illustrate the amount of water present the coefficient named K_{CP} was calculated:

$$K_{CP} = \frac{C}{C_{dry}}$$
(2)

where: C – the capacitance measured at 10 MHz while drying, C_{dry} – the capacitance of dry sample measured at 10 MHz

The amount of water absorbed by the HA layer was similar in all the samples. The initial values of K_{CP} were comparable but drying time was different. The drying time was determined as the moment when the K_{CP-1} dropped to 10% of its original value. Samples fabricated using lower torch power (200 and 300) which, as shown before, contain more crystalline phase in HA layer, had higher drying times which suggested that those samples had smaller pores of more complex structure.

5. Conclusions

Impedance spectroscopy appeared to be a suitable method for analysis of such complex structures as plasma sprayed HA coating. Elements used in equivalent circuit analysis were directly related to the separate areas in the layer. An increase of amorphous phase content with rise of spraying distance was observed.

The measurements of samples containing water allowed us to determine their porosity. Samples fabricated with lower spraying distance had a more complex pore

structure. This method seems to be very interesting but further investigations have to be performed, such as comparison with other structural (XRD, SEM, *etc*.) or porosity (BET, *etc*. [11]) techniques.

References

[1] PAWLOWSKI L., *Finely grained nanometric and submicrometric coatings by thermal spraying: A review*, Surface and Coatings Technology **202**(18), 2008, pp. 4318−4328.

[2] SOLTANI R., GARCIA E., COYLE T.W., MOSTAGHIMI J., LIMA R.S., MARPLE B.R, MOREAU C., *Thermomechanical behavior of nanostructured plasma sprayed zirconia coatings*, Journal of Thermal Spray Technology **15**(4), 2006, pp. 657−662.

[3] TOMASZEK R., NITSCH K., PAWŁOWSKI L., ZNAMIROWSKI Z., BRYLAK M., *Impedance spectroscopy of suspension plasma sprayed titania coatings*, Surface and Coatings Technology **201**(5), 2006, pp. 1930−1934.

[4] DOMARADZKI J., NITSCH K., PROCIOW E.L., KACZMAREK D., PASZKIEWICZ B., *Electrical characterisation of structures consisting of Ti−V−Pd thin film oxide on silicon by impedance spectroscopy*, Solid State Ionics **176**(25−28), 2005, pp. 2177−2180.

[5] FLEIG J., *Impedance spectroscopy on solids: The limits of serial equivalent circuit models*, Journal of Electroceramics **13**(1−3), 2004, pp. 637−644.

[6] JONSCHER A.K., *Universal Relaxation Law*, Chelsea Dielectric Press, London 1996.

[7] JORCIN J.-B., ORAZEM M.E., PÉBÈRE N., TRIBOLLET B., *CPE analysis by local electrochemical impedance spectroscopy*, Electrochimica Acta **51**(8−9), 2006, pp. 1473−1479.

[8] GITTINGS J.P., BOWEN C.R., DENT A.C.E., TURNER I.G., BAXTER F.R., CHAUDHURI J.B., *Electrical characterization of hydroxyapatite-based bioceramics*, Acta Biomaterialia **5**(2), 2009, pp. 743−754.

[9] RUSINIAK L., *Electric properties of water. New experimental data in the 5 Hz−13 MHz frequency range*, Acta Geophysica Polonica **52**(1), 2004, pp. 63−76.

[10] CATENACCIO A., DARUICH Y., MAGALLANES C., *Temperature dependence of the permittivity of water*, Chemical Physics Letters **367**(5−6), 2003, pp. 669−671.

[11] ROUQUEROL F., ROUQUEROL J., SING K., *Adsorption by Powders and Porous Solids. Principles, Methodology and Applications*, Academic Press, 1999.